A Study of Factors Affecting Wrist Channel Characteristics for Walking Postures using Motion Capture

Srijittra Swaisaenyakorn, Student Member, Steve Kelly, Member, and John C. Batchelor, Senior Member, IEEE

The link to this paper on IEEE Xplore® is

http://ieeexplore.ieee.org/xpl/articleDetails.jsp?tp=&arnumber=6714391&searchWithin%3Dp_First_Names%3AJ%26searchWithin%3Dp_Middle_Names%3AC%26searchWithin%3Dp_Last_Names%3ABatchelor%26ranges%3D2012_2014_p_Publication_Year%26matchBoolean%3Dtrue%26queryText%3D%28p_Authors%3ABatchelor%2C+J+C%29

The DOI is: 10.1109/TAP.2014.2300859

A Study of Factors Affecting Wrist Channel Characteristics for Walking Postures using Motion Capture

Srijittra Swaisaenyakorn, Student Member, Steve Kelly, Member, and John C. Batchelor, Senior Member, IEEE

Abstract—The creation of a 3D animated human model (avatar) to be used in Electromagnetic (EM) simulation software is described for low-outage Body Area Network applications such as healthcare. Scanned surface data of a human model is combined with movement data from a Motion Capture system to simulate an on-body channel between two Dual Band Metallic Button Antennas (DBMBAs) mounted on the wrist & chest and the wrist & hip during walking. An investigation of how different factors such as human geometry parameters, arm swing and wrist twisting can affect the body-centric channel during walking action is presented together with the relative significance of each of these factors on predicting body-centric channel gain.

Index Terms—Body area networks; Body centric communications; Motion capture

I. Introduction

Body area network (BAN) communication is becoming a popular technology for healthcare monitoring, car-driver interfacing, personal training systems, and mobile equipment for military personnel. Critical healthcare and military operation require low signal outage, and hence, it is important to identify and understand the factors causing changes in the characteristics of a BAN user's body. This not only prevents signal outage, but also extends battery life.

This paper presents a study of on-body channels during walking and comparison is made with other investigations, [1-10]. In [1-4] BAN studies were based on measurements on humans while [5] relied solely on EM simulations on a phantom. [6-10] included both measurement and simulation and [5-8] utilized proprietary numerical human phantoms and the animation package 'Poser' where physical stances were digitally posed and compared to video frames from the measurement.

However, in [5-8], it was difficult to ensure that the walking movement generated by posed phantoms was sufficiently close to that of the human under test. In [6] attempts were made to address this problem by having the human imitate the walking stances of the Poser model.

Also, knowing the exact locations and orientations of antennas in relation to the body surface is important and Motion Capture was used in [8] & by the authors in [9] to track the locations and orientations of antennas while [10] used markers to track arm movement during BAN measurements.

Manuscript received October 25, 2013. This work was supported by ESPRC under Grant EP/G055890/1.

The authors are with the School of Engineering, University of Kent, Canterbury, Kent, UK (phone: +441227827004; e-mail: ss638@kent.ac.uk, s.w.kelly@kent.ac.uk, j.c.batchelor@kent.ac.uk).

However, in [8] the antennas were represented as simplified point sources on a 'Poser' model. Finally, 60 GHz BANs were studied in [11] where the accuracy of the antenna locations and polarizations was critical due to narrow beamwidth, and motion capture was essential to locate the antennas.

The uncertainties of retrospectively matching a virtual phantom to human stances was first considered by the authors in [9] by creating an avatar closely representing the human under test and actual antenna positions were obtained by motion capture allowing accurate models to be included on the avatar.

BAN channel variation during walking has been studied for a single model in [1], [2], [4-8] and for a population of models in [3], [9], [10]. While [9] showed that a population with similar height had comparable forward transmission (S_{21}) levels for a given walking stance, differences between individuals were not negligible and could be up to 10dB. Consideration of the effect of variation in size and curvature of different humans has been shown in [12] and the human dimensional parameters and precise antenna placement considerations causing these variations will be expanded on here to inform future BAN channel predictions.

In section II, we outline the creation of 3D animated human models (avatars) for time domain simulation based on human surface scans and motion capture data. Section III demonstrates the advantage of the avatar over the HUGO model for on-body channel simulation while in section IV simulated results for the avatar with two body-centric antennas are validated by measurement. A study of various body parameters affecting on-body communication are given in Section V and Section VI concludes the paper.

II. Human Avatars Creation

The avatar creation process involves three main steps:

A. 3D body surface scan of the human under test

A person in a skin-tight suit was scanned with a 3 column optical laser 3D surface scanner with a density of 7 points/cm^2 [13], [14], Fig. 1.

B. Motion Capture during radio channel measurement

An 8 camera Vicon motion capture system tracked a human subject who wore 53 reflective markers. An animated skeleton representing the subject's movement together with the antenna locations was created.

Measurements were taken in an uncluttered 12m by 10.95m room of height 2.27m, Fig. 2. The room had a concrete floor, a metal ceiling and no furniture and the equipment operator was in a separate control room, Fig. 2.

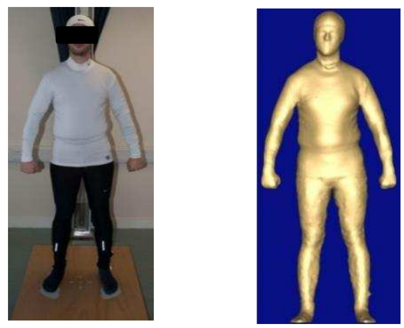

(a) (b)

Fig. 1. (a) 3D scan and (b) Body surface

Dual band Metalic Button Antennas (DBMBAs, [15]) were used for all measurements. These are top loaded monopoles on small ground planes with the appearance of denim jeans buttons and radiate at 2.45 and 5 - 6 GHz. While the scanned avatar model (a 168cm tall male) performed each posture, S_{21} and body movement data were captured by the network analyzer and the motion capture system. In order to capture the antenna positions and orientations they were mounted on plastic frames each with 5 reflective markers, Fig. 3. There was a 2 mm gap between the antennas and the skin and the antennas were connected via flexible cables to a Rohde & Schwarz FSH8 vector network analyzer with the settings in Table I.

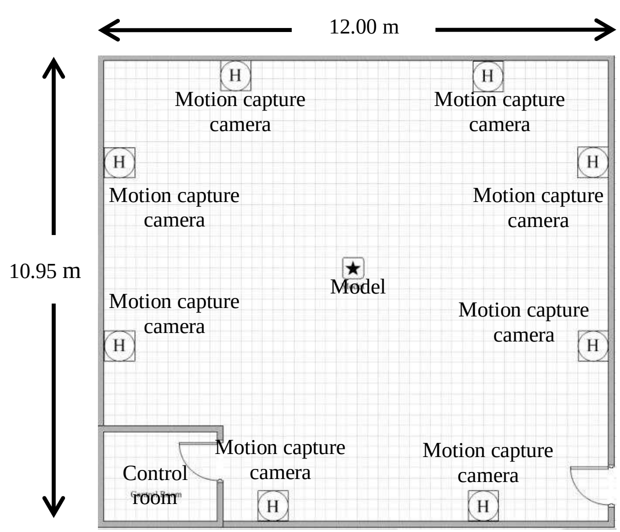

Fig. 2. Measurement room layout

The scanned body surface was imported into Autodesk Maya^{TM} and mapped to an articulated skeleton model. Captured movement data in the form of an animated skeleton was combined with the articulated skeleton and finally, the surface was converted to a solid using 'Mesh2Solid' software [16]. Further information on 3D character animation using motion capture can be found in [17].

TABLE I
EXPERIMENT AND SIMULATION SETTINGS

VNA settings		XFdtd simulation settings	
Frequency	1-6 GHz	Frequency	1-6 GHz
Output power	0 dBm	Mesh size	0.7-4 mm
VNA sweep time	625 ms	Absorbing boundaries	Perfectly matched layer
IF Bandwidth	10 kHz	Concrete floor dimension	0.25 x 18.43 x 0.008 m^3
Number of samples	631		

C. Avatar Tissue Material

Following the work of [6], [7], [18], an homogeneous tissue value of 2/3 that of muscle (ε_r = 35 and σ = 1.16 S/m) was used for the avatar and validated by S_{21} measurement at 2.45 GHz. The simulation used the parameters in Table I where the inclusion of a concrete floor was found to be necessary when antennas were mounted below the waist.

III. AVATAR COMPARISON WITH THE VISIBLE HUMAN PROJECT SIMULATED MALE (HUGO)

The detailed multi-tissue HUGO model [19] was compared with the avatar to establish the importance of accurate antenna positioning and body dimensions compared to detailed internal structure modeling.

Modeled antennas were placed on the right and left chest and Fig. 4 (a) shows the subject during measurement, while (b) depicts the avatar and HUGO models with chest antennas. Fig. 4 (c) and (d) show top views of the two cases and it is clear that the different body shapes significantly affect the antenna positions.

A set of 5 body mounted antenna pairs were measured as follows: right-left shoulders, right shoulder-left chest, right-left chest, right chest-right waist and left chest-right waist. Each measurement was repeated 5 times and the average result calculated. REMCOM XFdtd™ was used and Table II contains the simulated and the measured data at 2.45GHz. The error between measurement and simulation was less than 2.5dB for the avatar and up to 24dB for the HUGO model. The inaccuracy of the HUGO results is attributed to the difference between the actual and simulated antenna positions. In the case of the chest mounted antennas there is a 50° error between the HUGO antenna orientation and that of the avatar and inaccuracies were compounded due to signal reflection from HUGO's chin causing erroneous fading.

Additionally, when an antenna was mounted on the hip, error was introduced by the HUGO arm positions which did not correspond to the measurement subject, Fig. 5, and though the antenna orientations were close to measurement, arm blockage resulted in an error of greater than 12dB.

Fig. 3. A DBMBA mounted on a frame with 5 markers

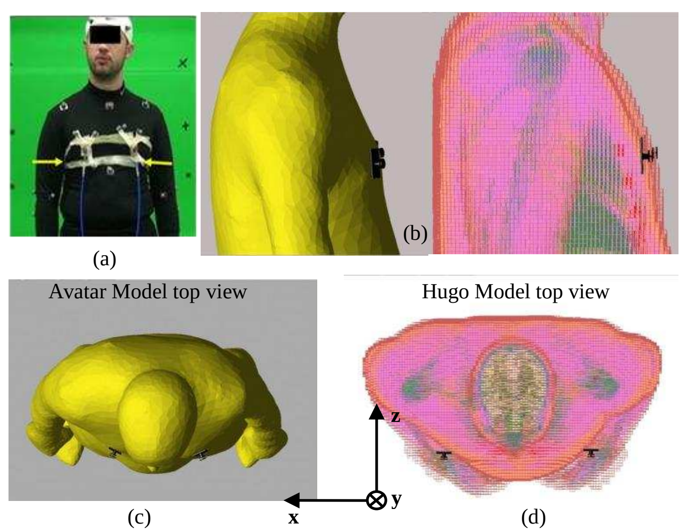

Fig. 4. (a) test model wearing chest antennas, (b) top view of antennas orientations relative to the avatar and HUGO model surface, (c) top view of avatar antenna positions and (d) top view of HUGO antennas

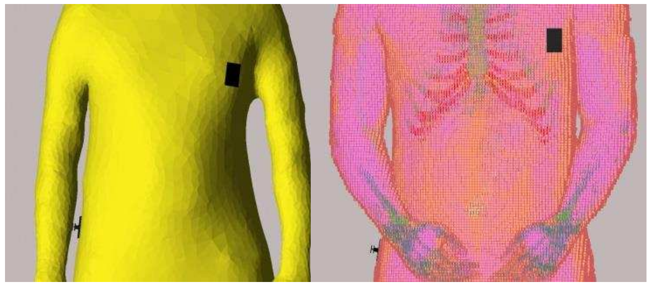

Fig. 5. Comparison of antennas positions on the avatar and the HUGO model for left chest–right waist case [20]

Therefore an avatar with body parameters and positions corresponding closely to measurement is significantly more accurate in terms of BAN channel simulation than an unrelated human with different dimensions.

IV. Walking Avatar On-Body Channel Simulation

Having established the accuracy of the avatar in a standing pose, the avatar was validated for walking positions. Two situations were considered where a DBMBA was placed on the right wrist for transmission to an identical antenna on (1) the left chest and (2) the right hip. These positions were chosen to represent communication from a wrist mounted sensor to a BAN hub gateway device mounted on the torso. The wrist–chest channel represents a challenging case, and the wrist to adjacent hip is a more favorable link condition. The wrist position is dynamic during walking and [3], [6], [8], [10] confirm that during walking wrist channels vary by 10dB or more due to depolarization and body shadowing. In [8] and [10] either the antenna or the arm position was tracked but neither study could track wrist twist since full motion capture was not used. However, the wrist angle is expected to be important for wrist mounted antennas and to assess this, a wrist channel was investigated for a walking cycle comprising 5 static steps as shown in Fig. 6. These steps are referred to as Positions 1 – 5.

A. Walking avatar channel simulation

A set of five measurements for each step position were taken and the average calculated to reduce multipath fading. The person performed a complete round of five steps, before starting the next set. Consistency in step size was assured by tape markers on the floor. A comparison of simulated and measured S_{21} for positions 1 - 5 at 2.45 and 5.50GHz were presented in [9]. In this paper, simulated S_{21} values are interpolated between the 5 steps to describe the effect of walking on the channel more fully. This was achieved by animating the avatar with motion capture data at intermediate positions between the 5 measured static positions.

TABLE II
S_{21} at 2.45GHz in Standing Position for Measurement and Simulation of 5 Different BAN Channels

	Measure-ment & Avatar	Hugo	Measure-ment & Avatar	Hugo	Measure -ment	Avatar	Hugo
Body mounted antenna positions	Actual antenna separation (cm)	Antenna separation error (cm)	Actual antenna tilt from (x, y z) axes	Antenna axis tilt error (x, y, z)	S_{21} (dB)	Simulated S_{21} minus measurement (dB)	Simulated S_{21} minus measurement (dB)
Right – Left Shoulder	30	6	57°, 3°, 3°	-26°, 5°, -3°	-44.8	-1.9	-4.7
Right Shoulder – Left Chest	32	8	77°, 27°, 61°	11°, -27°, 18°	-38.5	-2.4	-15.8
Right – Left Chest	19	9	2°, 50°, 4°	-2°, -50°, -3°	-25.0	-2.3	-24.8
Right Chest – Right Waist	32	8	2°, 77°, 1°	0°, 6°, 9°	-39.5	2.3	-9.3
Left Chest – Right Waist	44	9	2°, 114°, 4°	6°, 38°, 4°	-50.6	-0.8	-12.8

In total 12 intermediate points were captured and the simulated S_{21} is indicated by '✳' symbols in Fig. 7. The extrapolated avatar results compare well with measurement at the 5 key walking positions indicated by '◊' symbols.

In Fig. 7 (a), (right wrist–left chest) S_{21} starts to fall when the person begins to move into 'Position 2' (right leg forward) and increases again when 'Position 3' (left leg forward) is approached. When in position 2, the right wrist was behind the body causing torso blockage. For position 3 the model's right wrist was in front of the body so a line of sight (LOS) path existed at some arm swing angles.

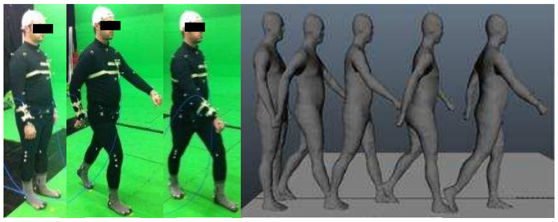

1 2 3 1 2 3 4 5

(a) (b)

Fig. 6. (a) S_{21} measurement of static walking postures for reference model with DBMBAs on right wrist and left chest (b) 3D animated avatar snapshot for 5 static walking stances

In Fig. 7 (b), (right wrist–right hip) S_{21} starts to rise when Positions 2 and 4 (right leg forward) are approached, and falls just before Positions 3 and 5 (left leg forward).

When in Position 2, the right wrist was behind the body and a LOS path existed, while in Position 3 the right wrist was forward and the path was shadowed by the arm. Measurement and simulation agree well with a difference of just 1.1 - 3.8dB for the wrist–chest link and 0.3 - 3.4dB for the wrist–hip and the overall average error is 2dB. This difference is partially due to the absence of a ceiling in the simulation. However, agreement is generally better than obtained in [6], [8] where 3dB and 5dB average differences were reported for studies in anechoic conditions. Therefore the accurate capture of antenna positions and body shape was observed to be more important than the detailed modeling of the surrounding environment.

B. Validation of walking avatar

To validate the simulated S_{21} data, the avatar results were compared with those taken independently by Rosini and D'Errico [3] where a similar movement regime, antenna type and locations on the body were used. Measured S_{21} was taken in [3] on a person walking 3m with two Top Loaded Monopoles (TLM) on (1) the left hand and chest and (2) the left hand and left hip.

Fig. 7 (a) includes a comparison of simulated S_{21} from our avatar and measurement from [3] for the wrist-chest channel and a good agreement is observed. A difference of up to 10dB exists in the positions between steps because the person in [3] had antennas on the left hand and left chest while the avatar had antennas on the right hand and left chest, therefore, body blockage was more significant for the avatar.

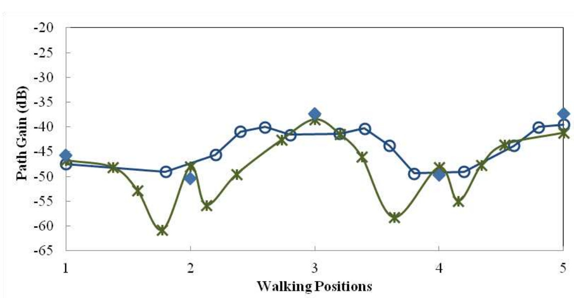

(a)

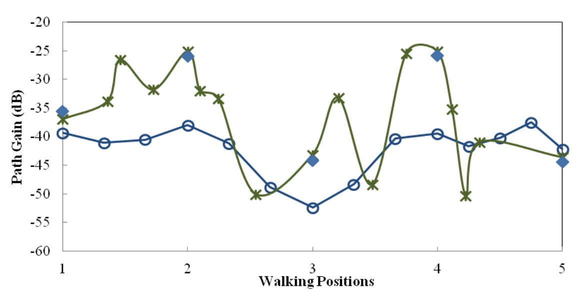

(b)

Fig. 7. Comparison of measured S_{21} (◊),simulated avatar S_{21} (✳) and measured from Rosini and D'Errico, [3], (o) for walking Positions 1 to 5 at 2.45 GHz. Antennas attached to (a) wrist and chest (b) wrist and hip

Fig. 7 (b) compares measurement from [3] with avatar simulation for the wrist–hip channel. Both show a similar trend when the wrist antenna is behind the body (Positions 2 and 4) and S_{21} increases due to forward radiation from the wrist antenna. Conversely, S_{21} reduces when the wrist is in front of the body (Positions 3 and 5) as rear radiation is required and arm blockage also occurs. The difference of up to 15dB between the avatar simulation and the measurement of [3] is primarily due to differences in degree of arm swing and wrist twist.

Although the walking avatar generally predicts on-body channel S_{21} for wrist to chest antennas within a few dB of measurement, a larger discrepancy was found in the wrist to hip case. For this channel the value of arm swing and wrist twist angles were more important with simulation confirming a 90° difference in wrist twist causes 14dB variation.

V. BAN Sensitivity to Body Parameters

In this section, an arm swing of 0° corresponds to arms hanging vertically while positive angles indicate the arm swings forward. A wrist twist of 0° means the wrist antenna faces front, 90° faces out from the side of the body and 180° faces to the rear.

A. The effect of torso dimensions on BANs

The effect on simulated S_{21} is shown in Fig. 8 for a wrist-to-chest and wrist-to-hip channels when a standing avatar torso was scaled independently in width and depth. The wrist antenna was facing forwards in all cases. Fig. 8 (a) shows the right wrist to left chest channel is quite stable with torso girth at both bands, though the channel gain decreases as the torso gets larger.

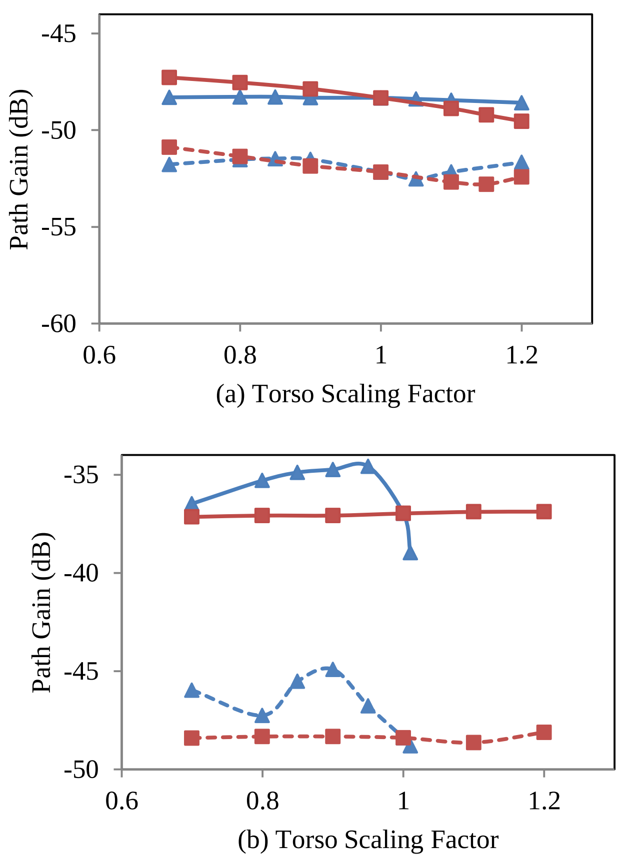

Fig. 8. Comparison of simulated S_{21} results for scaled avatar torso in width (Δ) and depth (□) for 2.45 GHz (solid lines) and 5.5 GHz (dashed line) in standing still position. Antennas locations: (a) wrist and chest (b) wrist and hip

Fig. 8 (b) illustrates the right wrist to right hip case. The channel is quite stable with torso depth (fat/thin) but a bigger influence occurs when the torso is narrow or wide as this alters the distance between the antennas. At 2.45GHz, channel gain increases for width scaling between 0.7 and 0.9 as constructive and destructive E-field interference occurs. Transmission starts to drop for scaled widths of 0.95 or more because the hip antenna moves into the area shadowed for the forward facing wrist antenna. A similar trend occurs at the 5.50GHz band except that a sharp drop in S_{21} occurs for a 0.8 width scaling factor. This is due to the more closely spaced interference nulls at the higher band. The torso cannot be scaled wider than 1.01 as the hip antenna begins to embed into the avatar wrist.

The variation in S_{21} with torso dimensions was not as large for the wrist to chest path as for the wrist to hip case because the former was always obscured by the body while the later was consistently Line of Sight.

B. The effect of wrist orientation and antenna positioning accuracy

Table III contains simulated data illustrating the S_{21} sensitivity to antenna separation from the skin of the wrist, the position of antenna across the wrist and the angle of wrist twist. The avatar was in a standing stance (Position 1, Fig. 6) with the wrist facing forwards (0°). Varying the antenna-skin separation between 0.1 and 10mm caused less than 1dB signal change meaning neither the wrist-hip nor the wrist-chest channels are particularly sensitive to antenna-skin separation due to the antenna rear ground plane.

There is some sensitivity in the wrist channels to antenna position with 10mm change across the wrist (keeping 0.1mm separation to the skin) leading to less than 2dB change. This indicates wrist mounted DBMBAs are not highly sensitive to separation and lateral position on a wrist. The wrist-hip channel is more strongly influenced by wrist twist than the wrist-chest channel, in the wrist-hip case 0 to 10° and 10° to 90° changes in wrist twist lead to 3dB and 14dB changes in S_{21} respectively at 2.45GHz. The wrist-chest channel is less sensitive to wrist twisting because the channel is partially obscured and depolarized by the torso which reduces the significance of antenna orientation.

TABLE III
SIMULATED S_{21} DEPENDENCE ON ANTENNA WRIST PLACEMENT AND WRIST ORIENTATION

	Parameter		Right wrist-left chest	Right wrist-right hip
	Study	Range	S_{21} change (dB)	S_{21} change (dB)
2.45 GHz	Wrist-antenna separation	0.1 to 10 mm	0.4	-0.7
	Antenna position across wrist	0 to 10 mm	-0.9	-1.5
	wrist twist	0 to 10°	0.1	2.7
	wrist twist	0 to 90°	-0.6	-14.3
5.5 GHz	Wrist-antenna separation	0.1 to 10 mm	0.6	0.6
	Antenna position across wrist	0 to 10 mm	1.2	-1.7
	wrist twist	0 to 10°	-0.6	0.8
	wrist twist	0 to 90°	1	-11.4

C. Walking group study

A population of 18 people with heights ranging from 153 to 184cm was recruited. The S_{21} results measured at 2.45GHz for the 18 individuals were plotted as scatter diagrams against various body parameters and a trend line found for each case. The trend line gradient was used as an indicator of parameter influence on the channel. For the right wrist to left chest case, Fig.9(a), the parameters associated with body dimensions (height, torso girth and arm length) are found to be relatively insignificant, while arm swing has a comparatively strong effect, both while standing and in step 1 (position 2). There is a certain amount of body blockage in both these instances which is significantly altered by arm swing angle. The extent of arm swing is less important for step 2 (position 3) as the antenna bearing arm is forward of the torso (line of sight) and the radiation pattern is broad. Wrist twist does not appear to influence the wrist-chest channel in any stance, presumably as the antenna pattern beam is broad in the plane of twist with the monopole null facing out from the side or the front of the body.

There is no body shadowing for the right wrist to right hip channel, Fig.10(a), and this case is strongly affected by the relative positions of the wrist and arm, therefore arm length, arm swing and wrist twist dominate, especially in step 2 (position 3). Arm swing is important in all 3 stances, while wrist twist only matters in step 2 (position 3). Arm length is more important in this channel than for wrist-to-chest due to standing wave interference between the arm and the torso so that relatively small antenna positional changes in the line of sight path lead to comparatively large changes in S_{21}.

The standard deviations for each parameter normalised by the parameter mean are presented, Figs. 9(b) and 10(b). As might be expected, for both channels, the largest spreads occur for the parameters of posture (arm swing and wrist twist) rather than physical dimensions (height, girth and arm length). It is encouraging to note in these two channels that within the ranges considered, physical body dimensions do not appear to affect the channel significantly, but, although a range of people of different heights was considered, the population did not include any obese individuals where the situation may have been different.

When comparing the avatar S_{21} of the previous section with the average measured S_{21} from the 18 person population, differences of just 1 – 2dB are found in the wrist–chest channel. For the wrist–hip case, bigger differences up to 7dB were observed meaning the avatar offered a better agreement in the NLOS wrist-chest case than the LOS wrist-hip.

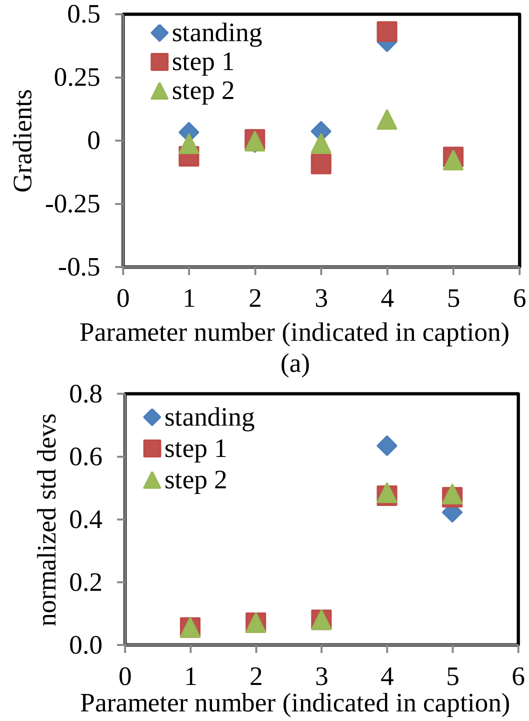

(b)

Fig. 9. Measured right wrist to left chest channel. Parameter 1 height, 2 torso girth, 3 arm length, 4 arm swing and 5 wrist twist respectively (a) parameter/S_{21} trend gradients plotted against parameters (b) parameter standard deviations normalised by parameter mean.

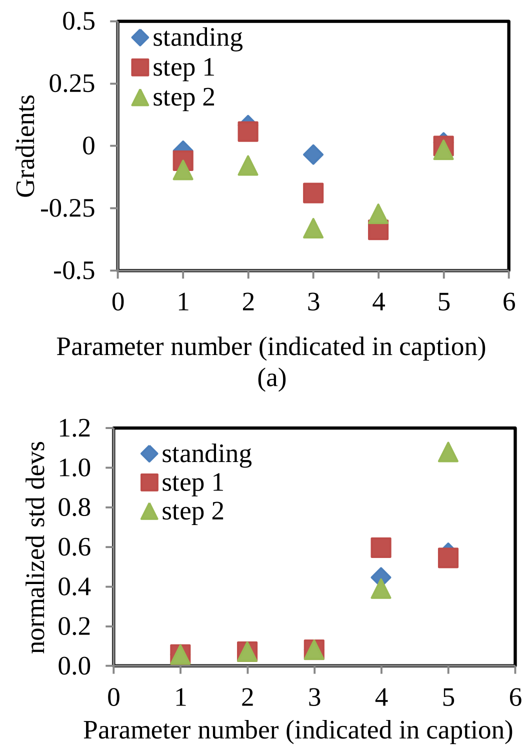

(b)

Fig. 10. Measured right wrist to right hip channel. Parameter 1 height, 2 torso girth, 3 arm length, 4 arm swing and 5 wrist twist respectively (a) parameter/S_{21} trend gradients plotted against parameters (b) parameter standard deviations normalised by parameter mean.

VI. CONCLUSIONS

A motion captured avatar based on actual test subjects has been shown to produce simulated BAN channel results ranging between 1 to 7dB from measurement. This data has been compared with that taken independently in [3] and good agreement was observed. A study of BAN channels on 18 people of various heights enabled various parameters to be separated and indicating that arm swing and to some extent wrist twist dominate physical body dimensions while walking. Instances where the body starts to block the channel path make the wrist mounted antenna position particularly important. While shadowing dominates S_{21} in the NLOS channel, the angle between antennas due to wrist twisting is a more significant factor in LOS channels and should be considered for wrist mounted body centric channel prediction. Above other differences in body geometry, the received signal most strongly depends on the co-polarization of the antennas.

Overall, with the use of motion capture and avatars, it has been possible to show the wrist-chest channel is more stable than the wrist-hip channel since significant body shadowing dominates the effect of smaller depolarisation losses due arm swing, wrist twisting and torso girth. The improved channel modelling arising from the avatar phantom developed in this paper has application in various BAN systems including healthcare, gaming and entertainment.

ACKNOWLEDGMENT

We acknowledge the UK Engineering and Physical Science Research Council for funding this work and Miss Swaisaenyakorn's studentship.

REFERENCES

[1] A. Taparugssanagorn, C. Pomalaza-Raez, R. Tesi, M. Hamalainen and J. Iinatti, "Effect of body motion and the type of antenna on the measured UWB channel characteristics in medical applications of wireless body area networks," in Ultra-Wideband, 2009. ICUWB 2009. IEEE International Conference on, 2009, pp. 332-336.

[2] S. L. Cotton and W. G. Scanlon, "An experimental investigation into the influence of user state and environment on fading characteristics in wireless body area networks at 2.45 GHz," Wireless Communications, IEEE Transactions on, vol. 8, pp. 6-12, 2009.

[3] R. Rosini and R. D'Errico, "Comparing on-body dynamic channels for two antenna designs," in Antennas and Propagation Conference (LAPC), 2012 Loughborough, 2012, pp. 1-4.

[4] D. Smith, L. Hanlen, D. Miniutti, Jian Zhang, D. Rodda and B. Gilbert, "Statistical characterization of the dynamic narrowband body area channel," in Applied Sciences on Biomedical and Communication Technologies, 2008. ISABEL '08. First International Symposium on, 2008, pp. 1-5.

[5] N. Haga and K. Ito, "Frequency dependence of on-body channels with top-loaded monopole antennas in the range of HF to UHF," in Microwave Conference, 2009. APMC 2009. Asia Pacific, 2009, pp. 2208-2211.

[6] P. S. Hall, Yang Hao, Y. I. Nechayev, A. Alomalny, C. C. Constantinou, C. Parini, M. R. Kamarudin, T. Z. Salim, D. T. M. Hee, R. Dubrovka, A. S. Owadally, Wei Song, A. Serra, P. Nepa, M. Gallo and M. Bozzetti, "Antennas and Propagation for On-Body Communication Systems," Antennas and Propagation Magazine, IEEE, vol. 49, pp. 41-58, 2007.

[7] Q. Wang, T. Tayamachi, I. Kimura and J. Wang, "An On-Body Channel Model for UWB Body Area Communications for Various Postures," Antennas and Propagation, IEEE Transactions on, vol. 57, pp. 991-998, 2009.

[8] T. Aoyagi, I. Iswandi, M. Kim, J. Takada, K. Hamaguchi and R. Kohno, "Body motion and channel response of dynamic body area channel," in Antennas and Propagation (EUCAP), Proceedings of the 5th European Conference on, 2011, pp. 3138-3142.

[9] S. Swaisaenyakorn, P.R. Young, S.W. Kelly and J.C. Batchelor, "Evaluation of 3D Animated Human Model from 3D Scanner and Motion Capture to be used in Electromagnetic Simulator for Body-Centric System," in the 5th International Conference on BioMedical Engineering and Informatics, Chongqing, China, 2012.

[10] L. Liu, R. D'Errico, L. Ouvry, P. De Doncker and C. Oestges, "Dynamic channel modeling at 2.4 GHz for on-body area networks," Advances in Electronics and Telecommunications-Radio Communication Series: Recent Advances in Wireless Communication Networks, vol. 2, 2011.

[11] Y. Nechayev, C. Constantinou, S. Swaisaenyakorn, O. Rakibet, J. Batchelor, P. Hall, C. Parini and J. Hunt, "Use of motion capture for path gain modelling of millimetre-wave on-body communication links," in Antennas and Propagation (ISAP), 2012 International Symposium on, 2012, pp. 987-990.

[12] K. Ali, A. Brizzi, S.L. Lee, Y. Hao, A. Alomainy and G.Z. Yang, "Numerical analysis of on-body channel for statistically-generated body shapes," Proceeding of Antennas and Propagation Conference (LAPC), Loughborough, UK, pp. 1-4, 2011.

[13] Human Solutions, "Body Scanner," http://www.human-solutions.com/fashion/front_content.php?idcat=126 (accessed on 16/01/2013).

[14] T. Lerch, M. MacGillivrary and T. Domina, "3D Laser Scanning: A Model of Multidisciplinary Research," Journal of Textile and Apparel, Technology and Management, North Carolina State University, vol. 5, pp. 1-22, Fall, 2007.

[15] B. Sanz-Izquierdo, F. Huang, J. C. Batchelor and M. I. Sobhy, "Study of single and dual band wearable metallic button antennas for personal area networks (PANs)," in Time Domain Methods in Electrodynamics, P. Russer and U. Siart, Eds. Springer-Verlag Berlin Heidelberg, 2008, pp. 173-187.

[16] Sycode, "Mesh To Solid - Software to Convert a Mesh to a Solid,"http://www.sycode.com/products/mesh_to_solid/index.htm (accessed on 16/01/2013).

[17] E. Lam, "Using mocap data driven skeletons to drive character controls,"http://www.cs.washington.edu/education/courses/cse460/05sp/links/Rigging/mocap_skels_drive_cons.htm (accessed on 23/05/2013).

[18] K. Ito, N. Haga, M. Takahashi and K. Saito, "Electric field distributions around the human body with a small antenna in the frequency range of 2.5 MHz to 2.5 GHz," in Antenna Technology, 2009. iWAT 2009. IEEE International Workshop on, 2009, pp. 1-4.

[19] C. Walby, The Visible Human Project: Informatic Bodies and Posthuman Medicine London: Routledge, 2000.

[20] S. Swaisaenyakorn and J. C. Batchelor, "Body gain study for animated human model in a body worn antenna system," in Antennas and Propagation (APCAP), 2012 IEEE Asia-Pacific Conference on, 2012, pp. 108-109.

Srijittra Swaisaenyakorn (S'11) received the B.Eng. degree in Electronics from the King's Mongkut Institute of Technology Ladkrabang, Bangkok, Thailand, in 2000 and M.Eng degree in Telecommunications from the Asian Institute of Technology, Pathumthani, Thailand, in 2002. In 2009, she received the M.sc. in Broadband and Wireless Communications from the University of Kent, Canterbury, Kent, U.K., where she is currently pursuing the Ph.D. degree in Electronics Engineering.

John C. Batchelor (S'93–M'95–SM'07) received the B.Sc. and Ph.D. degrees from the University of Kent, Canterbury, U.K., in 1991 and 1995, respectively. In 1997, he became a Lecturer with the Electronics Department, University of Kent, and a Senior Lecturer in 2006. He now heads the Antennas Group and was appointed to Reader in 2010. His research interests include body-centric and compact printed antennas, low frequency FSS and RFID tag design for passive wireless sensing and the Internet of Things.

Stephen W. Kelly (M'11) joined the University of Kent, Canterbury, U.K. in 1983 and is a senior lecturer in electronics as well as an honorary medical electronics specialist for the East Kent Hospitals University NHS Foundation Trust. He has worked for C&S Antennas Ltd on broadcast antennas and communications systems for the U.K. Government Home Office. His current research interests include medical electronics, multi-parameter instrumentation for clinical Speech & Language Therapy, telemedicine and computer-based assessment of clinical conditions.